

1992

Measurement of the Coefficient of Thermal Expansion of Superconducting Thin Films Using Powder X-Ray Diffraction

Biju Chandran

University of Arkansas, Fayetteville


R. Calvin Goforth

University of Arkansas, Fayetteville

S. Nasrazadani

University of Arkansas, Fayetteville

Follow this and additional works at: <http://scholarworks.uark.edu/jaas>

 Part of the [Heat Transfer, Combustion Commons](#), and the [Other Materials Science and Engineering Commons](#)

Recommended Citation

Chandran, Biju; Goforth, R. Calvin; and Nasrazadani, S. (1992) "Measurement of the Coefficient of Thermal Expansion of Superconducting Thin Films Using Powder X-Ray Diffraction," *Journal of the Arkansas Academy of Science*: Vol. 46 , Article 39. Available at: <http://scholarworks.uark.edu/jaas/vol46/iss1/39>

This article is available for use under the Creative Commons license: Attribution-NoDerivatives 4.0 International (CC BY-ND 4.0). Users are able to read, download, copy, print, distribute, search, link to the full texts of these articles, or use them for any other lawful purpose, without asking prior permission from the publisher or the author.

This Article is brought to you for free and open access by ScholarWorks@UARK. It has been accepted for inclusion in Journal of the Arkansas Academy of Science by an authorized editor of ScholarWorks@UARK. For more information, please contact scholar@uark.edu.

MEASUREMENT OF THE COEFFICIENT OF THERMAL EXPANSION OF SUPERCONDUCTING THIN FILMS USING POWDER X-RAY DIFFRACTION

BIJU CHANDRAN, R. CALVIN GOFORTH, and S. NASRAZADANI

Department of Mechanical Engineering
University of Arkansas
Fayetteville, AR 72701

ABSTRACT

The High Density Electronics Center (HiDEC) at the University of Arkansas, Fayetteville is developing the technology for High Temperature Superconductor Multi-Chip Modules (HTSC-MCM's). As part of this work, we are looking at the mechanical properties of HTSC materials. An important mechanical property which influences the mechanical integrity of the hybrid MCM is the coefficient of thermal expansion (CTE) of the HTSC films. As a first step in developing a procedure for the determination of the CTE of HTSC materials, the lattice parameters and the CTE of an α -alumina substrate have been determined by powder x-ray diffraction technique. An extension of this technique applicable to HTSC materials is presented.

INTRODUCTION

The goal of the research presented here is to determine the lattice parameters and the CTE of high temperature perovskite superconductors. These materials are being developed by HiDEC for use as signal propagation layers and interconnects in high temperature superconducting MCM's.

Multi-chip modules represent the next stage in the continual evolution of higher-density, higher-speed electronic packaging technologies. With the clock rates of new generation computers increasing, the chip-to-chip interconnection paths become the limiting factor in system performance. In an MCM, discrete IC packages are eliminated by placing the bare IC's as close as possible on a high density interconnect substrate. One limitation of conventional MCM's is that as the size of the MCM increases, at a constant chip placement density, the average interconnect length increases. If the number of chip rows is increased from 1 to 20 on a square MCM, the average interconnect length will increase by about 35% from 3.1 to 4.2 chip pitches. As a result, wider and thicker material traces are required to avoid excessive resistance. To accommodate these larger cross-section interconnects, conventional MCM'S must be made with multiple signal layers, with an accompanying increase in complexity and resultant lower product yields. High temperature superconductor MCM's do not need large cross-section interconnects. Signal propagation delays are also reduced. For 10 GHz operation, a 30 cm copper interconnect line would need to be approximately 35 microns wide compared to less than 2 microns wide for a superconducting interconnect. For superconducting MCM's, two signal layers should always be sufficient. Figure 1 shows a cross-sectional schematic of a superconducting MCM.

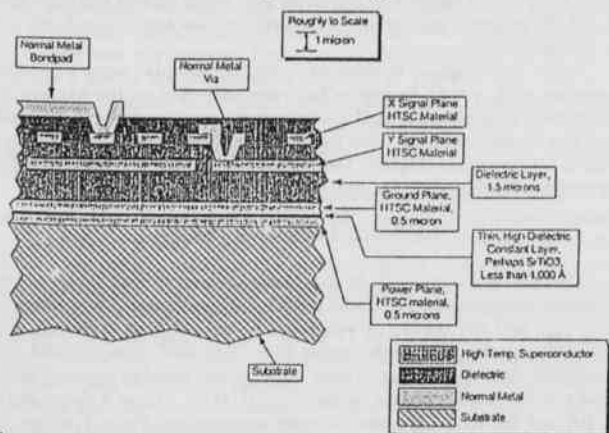


Figure 1. Schematic of a HTSC MCM.

A number of key issues need to be addressed before high temperature superconducting MCM's can be successfully fabricated. Superconducting MCM's will require the integration of high temperature superconductors with several materials (insulators, semiconductors, and metals) (Markstein, 1991). Hence, understanding interfacial effects are of crucial importance. The constraints imposed by mismatch of lattice constants between the superconducting material and the substrate need to be known before the mechanical stability of such a multilayered structure can be determined accurately. Also, the difference in the coefficient of thermal expansion between the superconducting material and the substrate can cause cracking during thermal cycling. Since the mechanical properties, including the coefficient of thermal expansion, of many of the high temperature superconducting materials are not well known, it is important that the mechanical properties be characterized. We have begun work to measure the CTE of HTSC thin films using a powder x-ray diffraction technique. We have initially used α -alumina samples, for which the CTE is known, in order to verify the technique.

THEORY AND CALCULATIONS

The phenomenon of x-ray diffraction by crystals results from a scattering process in which the x-rays are scattered by the electrons of the atom without change in wavelength. A diffracted beam is produced by such scattering when certain geometric conditions are satisfied (expressed as the Bragg law or the Laue equations) (Klug and Alexander, 1954). Figure 2 shows a schematic of x-ray diffraction on a crystalline sample.

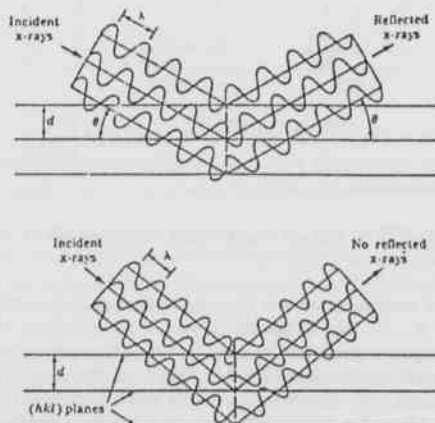


Figure 2. Schematic of the x-ray diffraction technique.

Measurement of the Coefficient of Thermal Expansion of Superconducting Thin Films

The resulting diffraction pattern of a crystal, comprising both the positions and the intensities of the diffraction effects, is a fundamental physical property of the substance. Analysis of the positions of the diffraction peaks leads to the determination of the size, shape, and orientation of the unit cell. The Bragg equation for a crystal is commonly expressed as

$$n\lambda = 2d \sin(\theta) \quad (1)$$

For a crystal of a given inter-planar spacing d , and for a given wavelength λ , the various order n of reflection occur only at the precise values of angle θ which satisfy the Bragg equation, and these angles correspond to a particular hkl plane (Miller indices) of the crystal being studied. At other angles there is no reflected beam because of interference.

There are a number of techniques that can be applied for the precise calculation of the unit-cell dimensions (lattice parameters) from the positions of the different hkl peaks of a powder diffraction pattern. The accuracy of each technique depends on the nature of the hkl peak and the angular positions of the peaks used. For example, the Straumanis technique can be used to determine a_0 values accurately if hk0 peaks near $\theta = 90^\circ$ are used, and c_0 values accurately if 001 peaks near $\theta = 90^\circ$ are used for their calculation (Peiser and Rooksey, 1960). A good technique to use for the case where there are a number of diffraction peaks in the angular range from $\theta = 60^\circ$ to 90° is the Cohen's least squares method (Peiser and Rooksey, 1960). This is the technique we are using to determine lattice parameters.

The quadratic form of the Bragg equation for a hexagonal crystal can be written as

$$\frac{\lambda^2}{3a_0^2} (h^2 + hk + k^2)_i + \frac{\lambda^2}{4c_0^2} l_i^2 = \sin^2\theta \quad (2)$$

To account for the combined action of the systematic errors, an error term ($D \sin^2 2\theta$) is added to equation (2) to get

$$\frac{\lambda^2}{3a_0^2} (h^2 + hk + k^2)_i + \frac{\lambda^2}{4c_0^2} l_i^2 + D \sin^2 2\theta = \sin^2\theta \quad (3)$$

The meaning of equation (3) is that the observed $\sin^2\theta$ value for any line above $\theta = 60^\circ$ will be in error by an amount equal to $D \sin^2 2\theta$ as a result of the combined action of the systematic errors (for any line above $\theta = 30^\circ$ the combined action of the systematic errors would amount to an error term of $D \sin^2(2\theta)[1/\sin(\theta) + 1/(\theta)]$).

As a result of the random observational errors, however, equation (3) will not hold exactly for any particular reflection, but will vary by a small amount v_i . The procedure for evaluating the lattice parameters by the least squares technique consists of minimizing the effect of the random observational errors given by

$$\sum v_i^2 = \left[\frac{\lambda^2}{3a_0^2} (h^2 + hk + k^2)_i + \frac{\lambda^2}{4c_0^2} l_i^2 + D \sin^2 2\theta - \sin^2\theta \right]^2 \quad (4)$$

Substituting

$$A_0 = \frac{\lambda^2}{3a_0^2} \quad B_0 = \frac{\lambda^2}{4c_0^2} \quad (5)$$

and

$$\alpha_i = (h^2 + hk + k^2)_i \quad \beta_i = l_i^2 \quad \delta_i = \sin^2 2\theta_i \left[\frac{1}{\sin\theta_i} + \frac{1}{\theta_i} \right] \quad (6)$$

equation (4) reduces to

$$\sum v_i^2 = \sum [A_0 \alpha_i + B_0 \beta_i + D \delta_i - \sin^2\theta_i]^2 \quad (7)$$

For minimum random error, the first derivatives of $\sum v_i^2$ with respect to the variables A_0 , B_0 , and D should be zero. The advantage of the least squares technique is that it can be used on any diffraction pattern as long as there are sufficient number of lines to get a good average value of the lattice parameters. The disadvantage is that equal importance is given to reflections at all angles. This method will give accurate results when the lines near $\theta = 90^\circ$ are used to calculate the lattice parameters. The derivatives of equation (7) give the three normal equations (8):

$$A_0 \sum \alpha_i^2 + B_0 \sum \alpha_i \beta_i + D \sum \alpha_i \delta_i = \sum \alpha_i \sin^2\theta_i \quad (8a)$$

$$A_0 \sum \beta_i \alpha_i + B_0 \sum \beta_i^2 + D \sum \beta_i \delta_i = \sum \beta_i \sin^2\theta_i \quad (8b)$$

$$A_0 \sum \delta_i \alpha_i + B_0 \sum \delta_i \beta_i + D \sum \delta_i^2 = \sum \delta_i \sin^2\theta_i \quad (8c)$$

These can be solved for A_0 , B_0 , and D . The lattice parameters a_0 and c_0 can then be calculated from equations (5), where the wavelength λ of the incident radiation is known.

In the case of an orthorhombic crystal, the normal equations which would give a minimum value of the random errors are given by equations (9):

$$\sum \alpha_i (A_0 \alpha_i + B_0 \beta_i + C_0 \gamma_i + D \delta_i - \sin^2\theta_i) = 0 \quad (9a)$$

$$\sum \beta_i (A_0 \alpha_i + B_0 \beta_i + C_0 \gamma_i + D \delta_i - \sin^2\theta_i) = 0 \quad (9b)$$

$$\sum \gamma_i (A_0 \alpha_i + B_0 \beta_i + C_0 \gamma_i + D \delta_i - \sin^2\theta_i) = 0 \quad (9c)$$

$$\sum \delta_i (A_0 \alpha_i + B_0 \beta_i + C_0 \gamma_i + D \delta_i - \sin^2\theta_i) = 0 \quad (9d)$$

Here,

$$A_0 = \frac{\lambda^2}{4a_0^2} \quad B_0 = \frac{\lambda^2}{4b_0^2} \quad C_0 = \frac{\lambda^2}{4c_0^2} \quad (10)$$

and

$$\alpha_i = h_i^2, \quad \beta_i = k_i^2, \quad \gamma_i = l_i^2, \quad \delta_i = \sin^2 2\theta_i \left[\frac{1}{\sin\theta_i} + \frac{1}{\theta_i} \right] \quad (11)$$

In the present work, equations (8) were used to calculate A_0 , B_0 , and D values and equations (5) was used to calculate the lattice parameters a_0 and c_0 .

EXPERIMENTAL SETUP

Initial lattice parameter and CTE measurements indicated that the resolution and repeatability that could be obtained using a strip chart to record the diffraction peaks was poor. A small percentage difference (3.1% difference in a_0 and 2.5% difference in c_0) in lattice parameter measurements during two different runs with the same conditions caused an error of more than an order of magnitude in the CTE values. Therefore, a computer data acquisition system was added to the diffractometer. An incremental optical encoder with a disc resolution of 5000 pulses per revolution was attached to a micrometer shaft of the goniometer. The micrometer shaft is attached to the goniometer table by a tightly fitting worm gear and makes a complete revolution per degree turn of the goniometer shaft. We therefore obtain an encoder pulse every 0.72 arc-second turn of the goniometer table. An IBM PC compatible computer data acquisition board with a clock counter and 8-channel 16 bit analog to digital converter is used for the data acquisition. The clock counter of the board is used to count pulses from the encoder. The voltage output from the detector of the diffractometer, which corresponds to the amplitude of the reflected x-rays (the y-axis in a strip chart recording) is read by the A/D converter after being filtered and amplified. A BASIC program was written to control the data acquisition board and to process the data.

Two 1 inch square α -alumina substrate samples were cemented together with a strip heater in between and used as the sample for diffraction analysis. A type K thermocouple was cemented to the back surface of the assembly, and the temperature was measured using a digital thermocouple display. Temperature of the sample was controlled by varying the current to the strip heater.

RESULTS AND DISCUSSION

The diffraction pattern of the alumina sample was taken at two different temperatures: 27°C and 108°C. The goniometer 2θ rate was set at $1^\circ/\text{min}$ and the specimen subjected to copper K- α radiation. Ten diffraction peaks between the angles $2\theta = 70$ to 120° were recorded. The computer data acquisition system enabled the angular position at the peaks to be recorded with a resolution of 0.0002°. Figure 3 shows the [1 2 10] and the [0 0 12] peaks at room temperature. Table 1 shows the angular positions of the hkl peaks at the two different temperatures. The

Biju Chandran, R. Calvin Goforth, and S. Nasrazadani

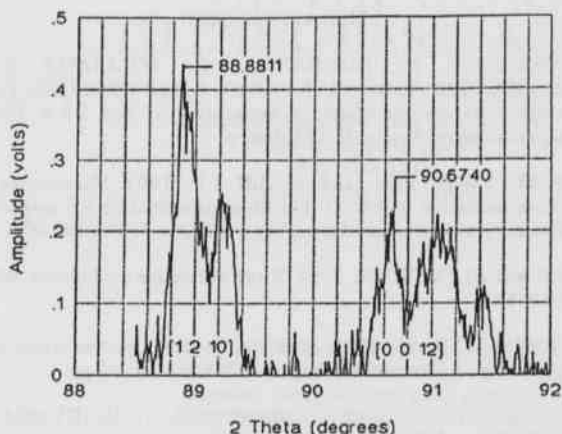


Figure 3. [1 2 10] and [0 0 12] peaks of α -alumina at room temperature.

Table 1. Observed and corrected 2 θ positions at different hkl planes.

hkl	2 θ_{obs} 24°	2 θ_{cor} 24°	2 θ_{obs}	2 θ_{cor}	2 θ_{cor}
1 0 10	76.7423	76.7918	76.7369	76.7423	76.7918
3 1 2	86.4026	86.4521	86.3429	86.3483	86.3978
1 2 10	88.8811	88.9306	88.8350	88.8404	88.8899
0 0 12	90.6740	90.7235	90.5961	90.6015	90.6509
2 2 6	95.1822	95.2317	95.1741	95.1795	95.2290
1 2 10	101.117	101.1665	101.0388	101.0442	101.0937
3 1 8	111.1274	111.1769	110.975	110.9804	111.0299
3 2 4	116.2100	116.2595	116.1832	116.1886	116.2381
1 1 4	116.6462	116.6957	116.5974	116.6028	116.6523
4 1 0	117.9938	118.0433	117.9896	117.9950	118.0445

goniometer does not return precisely to the same starting angle at each run. To account for any starting angle offset between the two runs, the [1 0 10] peak (at $2\theta=76^\circ$) was recorded at the same temperature during both runs. During the high temperature run, the [1 0 10] peak was recorded at 24°C , and the strip heater was turned on to heat the sample uniformly to 108°C before proceeding to the next hkl peak at approximately 86° . The difference between the angular positions of the [1 0 10] peaks at the two different temperatures was used as a starting angle offset to correct the angular positions obtained during the high temperature run ($76.7423 - 76.7369 = .0054^\circ$). This technique is applicable because all the other errors associated with the x-ray diffraction method, namely absorption and eccentricity errors, remained the same for the two different runs since the sample was not removed from the sample holder between the runs. Column 2 shows the 2θ positions recorded at $T=24^\circ\text{C}$, and Column 4 shows those recorded at $T=108^\circ\text{C}$ without the offset correction. Column 5 shows the 2θ values at 108°C corrected for a starting offset of 0.0054° . Here the starting angle offset for the data at room temperature data was neglected.

The lattice parameters a_0 and c_0 were calculated from ASTM published data (Smith and Berry, 1960) using Cohen's least square technique ($a_0 = 4.7295 \text{ \AA}$ and $c_0 = 13.0838 \text{ \AA}$). These lattice parameter values were used to calculate the correct position of the [1 0 10] peak. This was found to be 76.7918° . The difference ($76.7918 - 76.7423$) of 0.0495° was used as an offset to correct the room temperature 2θ readings. The 2θ readings at $T=108^\circ\text{C}$ was corrected with the new starting offset value ($79.7918 - 76.7369 = 0.0549$) calculated from the corrected room temperature readings. The corrected room temperature 2θ readings and the corresponding 2θ values at 108°C are shown in Columns 3 and 6, respectively.

The lattice parameters were calculated for the uncorrected 24°C 2θ

readings (Column 2) and the 2θ readings at 108°C (Column 5) using the 9 diffraction peaks above 80° . The [1 0 10] peak at 24°C was not used so that the same degree of accuracy could be maintained for the lattice parameters calculated at the two different temperatures.

The normal equations calculated for the room temperature data in column 2 are:

$$1391A_0 + 3068B_0 + 200.5646D = 60.3804$$

$$3068A_0 + 46656B_0 + 1172.656D = 269.6669$$

$$200.5646A_0 + 1172.656B_0 + 46.7089D = 11.8169$$

The lattice parameters calculated from these equations are $a_0 = 4.6988 \text{ \AA}$, and $c_0 = 13.1736 \text{ \AA}$. The lattice parameters calculated for the 108°C data in Column 5 are $a_0 = 4.6996 \text{ \AA}$, and $c_0 = 13.1834 \text{ \AA}$. The CTE is then given by

$$a\text{-axis CTE} = \frac{(4.69962 - 4.69881)}{4.69881 \times 84} = 2.04888 \times 10^{-6} / ^\circ\text{C}$$

$$c\text{-axis CTE} = \frac{(13.18344 - 13.17359)}{13.17359 \times 84} = 8.89915 \times 10^{-5} / ^\circ\text{C}$$

The average CTE is therefore $5.474 \times 10^{-6} / ^\circ\text{C}$.

The lattice parameters and the CTE were similarly calculated from the room temperature 2θ values corrected with the starting offset, and the correspondingly corrected 2θ readings at 108°C . The CTE obtained using these data is $5.4669 \times 10^{-6} / ^\circ\text{C}$, which is almost the same as the CTE calculated using the data without the room temperature data corrected for the starting error. Therefore, a small common offset on the two sets of data does not appear to introduce a significant error in the calculated CTE. The CTE value was compared to the published value of $6.3 \times 10^{-6} / ^\circ\text{C}$ (Shackelford, 1992). The CTE calculated using X-ray diffraction is found to be about 13% lower than the published value. One possible reason for this is that the incident x-ray is not entirely K- α , but a mixture of different copper radiations. This produced multiple peaks (one for every

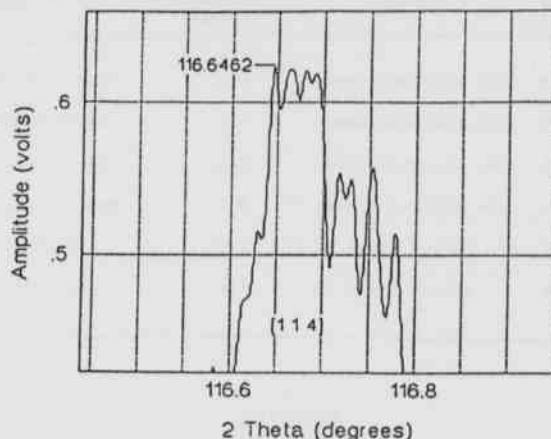


Figure 4. Magnified view of the multiple [1 1 4] peaks of α -alumina.

wavelength) at each peak location, as can be seen in Figure 4. It is possible that we recorded different wavelength peaks at some peak positions during the two runs. Also, we do not know how much sample-to-sample CTE variation exists in α -alumina.

DIRECTION OF FUTURE WORK

Superconducting thin films are deposited on substrates with their c-axis normal to the substrate surface. Since x-ray diffraction only gives diffraction lines for planes parallel to the surface, it is only possible to

calculate c_0 (normal to the film surface), and hence the CTE along the c-axis, for an HTSC film as deposited. We are primarily interested in the CTE along the plane of the film surface (a-axis CTE for hexagonal crystal, a-axis and b-axis CTE's for an orthorhombic crystal) since the thermal stress at the thin film and substrate interface will be due to the CTE mismatch parallel to the film surface. Therefore, we are developing a procedure to determine the lattice parameters from diffraction measurements of a pulverized HTSC thin film slurry. Similar procedures have been successfully applied elsewhere (Mizutani *et al.*, 1976). The thin film along with a small portion of the substrate is finely pulverized. The powder needs to be finely ground in order to reduce absorption errors. The powder is then made into a slurry with methanol and pasted on a quartz sample holder. Some HTSC powder absorb moisture and this can cause the diffraction pattern to change. In such cases, a mixture of toluene and vaseline can be used instead of methanol (Doverspike *et al.*, 1991). If the lattice parameters of the substrate have been previously determined, then the diffraction lines of the substrate can act as an internal standard (Peiser and Rooksey, 1960). Since the errors associated with both the powders are the same, the error associated with the substrate's lattice parameters can be determined and the error can be used as a correction factor for the calculated thin film lattice parameters. If the substrate's lattice parameters are not known accurately, then some high purity silicon powder can act as a standard (Mizutani *et al.*, 1976). The diffraction pattern needs to be taken over a large angular range, since the errors associated with x-ray diffraction decrease as the incident angle approaches 90° . Most of the HTSC materials have strong high angle peaks (Yvon and Francois, 1989), (Ece *et al.*, 1991), (Tonouchi *et al.*, 1987), (Zhou *et al.*, 1988).

At this stage of the work, we have verified the x-ray diffraction technique for the determination of the CTE of an alumina sample. We will now measure the CTE of some slurried thin films with well known properties in order to verify the HTSC sample preparation technique described above. Finally, we will use the methods to measure the CTE's of a variety of YBCO and thallium - based HTSC thin films.

LITERATURE CITED

- DOVERSPIKE, K., HUBBARD, C.R., WILLIAMS, R.K., ALEXANDER, K.B., BRYNESTAD, J., and KROEGER, D.M., 1991. Anisotropic thermal expansion of the 1:2:4 YBCO superconductor. *Physica C*. 172. 486 pp.
- ECE, M., VOOK, R.W., and ALLEN, J.P., 1991. Microstructural characterization of YBCO thin films deposited by RF magnetron sputtering as a function of annealing conditions. *J. Mat. Res.*6(2).
- KLUG and ALEXANDER. 1954. X-ray diffraction procedures. Wiley. New York.
- MARKSTEIN, H. W., 1991. Multichip modules pursue wafer scale performance. *Electronic Packaging and Production*. 40 pp.
- MIZUTANI, T., OHSAWA, J., NISHINAGA, T., UCHIYAMA, S., 1976. Thermal expansion coefficient of boron monophosphide. *Jpn. J. Appl. Phys.* 15(7). 1305 pp.
- PEISER, H. S., and ROOKSEY, H. P., 1960. X-ray diffraction by polycrystalline materials. Chapman & Hall. New York.
- SHACKELFORD, J. F., 1992. Introduction to materials science for engineers. Macmillan. New York.
- SMITH, J. V., and BERRY, L. G., (eds.) 1960. X-ray powder diffraction data file. ASTM. Philadelphia.
- TONOUCHI, M., YOSHIZAKO, Y., TAKAHASHI, T., SAKAGUCHI, KITA, S., FUJIWARA, Y., and KOBAYASHI, T., 1987. High T_c superconductivity of RF sputtered Er-Ba-Cu-O films. *Jpn. J. Appl. Phys.* 26(9). L1462 pp.
- YVON, K. and FRANCOIS, M. 1989. Crystal structure of HTSC oxides - Review article 1987-1988. *Z. Phys. B*. 76. 413 pp.
- ZHOU, J., ICHIKAWA, Y., ADACHI, H., MITSUYU, T., and WASA, K., 1988. Preparation of $Tl_1Ba_2Ca_3Cu_4O_x$ thin films by RF magnetron sputtering. *Jpn. J. Appl. Phys.* 27(12). L2321 pp.